VILNIUS UNIVERSITY
SEMICONDUCTOR PHYSICS INSTITUTE OF
CENTER FOR PHYSICAL SCIENCES AND TECHNOLOGY

Česlav Paškevič

INVESTIGATION OF ELECTRIC PROPERTIES OF SEMICONDUCTOR HETEROSTRUCTURES FOR MICROWAVES ELECTRONICS

Summary of doctoral dissertation
Physical sciences, physics (02 P), semiconductor physics (P 265)

Vilnius, 2012

Doctoral dissertation was prepared at Semiconductor Physics Institute of Center for Physical sciences and technology in 2006–2011

Scientific supervisor:

Prof Dr Habil Steponas Ašmontas (Semiconductor Physics Institute of Center for Physical sciences and technology, physical sciences, physics – 02 P, semiconductor physics – P 265

Consultants:

Prof Dr Algirdas Sužiedėlis (Semiconductor Physics Institute of Center for Physical sciences and technology, physical sciences, physics – 02 P, semiconductor physics – P 265

Prof Dr Habil Algis Jurgis Kundrotas (Semiconductor Physics Institute of Center for Physical sciences and technology, physical sciences, physics – 02 P, semiconductor physics – P 265)

The Vilnius University Doctoral Dissertation Committee in Physics:

Chairman:

Prof Dr Habil Saulius Balevičius (Semiconductor Physics Institute of Center for Physical sciences and technology, physical sciences, physics – 02 P, semiconductor physics – P 265)

Members:

Prof Dr Habil Gytis Juška (Vilnius University, physical sciences, physics – 02 P, semiconductor physics – P 265)

Prof Dr Vytautas Kleiza (Kaunas Technology University, physical sciences, informatics – 09 P, mathematical and general theoretical physics, classical mechanics, quantum mechanics, relativity, gravitation, statistical physics, thermodinamics – P 190)

Prof Dr Habil Romualdas Navickas (Vilnius Gediminas Technical University, technological sciences, electrical and electronic engineering – 01 T, microelectronics – T 171)

Prof Dr Habil Antanas Feliksas Orliukas (Vilnius University, physical sciences, physics – 02 P, semiconductor physics – P 265)

Opponents:

Prof Dr Habil Adolfas Dargys (Semiconductor Physics Institute of Center for Physical sciences and technology, physical sciences, physics – 02 P, semiconductor physics – P 265)

Prof Dr Habil Eugenijus Šatkovskis (Vilnius Gediminas Technical University, physical sciences, physics – 02 P, semiconductor physics – P 265)

The doctoral dissertation will be defended at the public meeting of Council of Scientific Field of Physics at 4 p.m. on September 13, 2012 in the conference hall of Semiconductor Physics Institute of Center for Physical sciences and technology, A. Goštauto st. 11, LT–01108 Vilnius, Lithuania.

The summary of the doctoral dissertation has been mailed out on the 13th of August, 2012.

The doctoral dissertation is available for review at the libraries of Center for Physical sciences and technology and Vilnius University.

VILNIAUS UNIVERSITETAS
FIZINIŲ IR TECHNOLOGIJOS MOKSLŲ CENTRO
PUSLAIDININKIŲ FIZIKOS INSTITUTAS

Česlav Paškevič

PUSLAIDININKINIŲ ĮVAIRIATARPIŲ DARINIŲ, SKIRTŲ MIKROBANGŲ ELEKTRONIKAI, ELEKTRINIŲ SAVYBIŲ TYRIMAS

Daktaro disertacijos santrauka
Fiziniai mokslai, fizika (02 P), puslaidininkių fizika (P 265)

Vilnius, 2012

Disertacija rengta 2006–2011 metais Fizinių ir technologijos mokslų centro Puslaidininkių fizikos institute

Mokslinis vadovas:

prof. habil. dr. Steponas Ašmontas (Fizinių ir technologijos mokslų centro Puslaidininkių fizikos institutas, fiziniai mokslai, fizika – 02 P, puslaidininkių fizika – P 265)

Konsultantai:

prof. dr. Algirdas Sužiedėlis (Fizinių ir technologijos mokslų centro Puslaidininkių fizikos institutas, fiziniai mokslai, fizika – 02 P, puslaidininkių fizika – P 265)

prof. habil. dr. Algis Jurgis Kundrotas (Fizinių ir technologijos mokslų centro Puslaidininkių fizikos institutas, fiziniai mokslai, fizika – 02 P, puslaidininkių fizika – P 265)

Disertacija ginama Vilniaus universiteto fizikos mokslo krypties taryboje:

Pirmininkas:

prof. habil. dr. Saulius Balevičius (Fizinių ir technologijos mokslų centro Puslaidininkių fizikos institutas, fiziniai mokslai, fizika – 02 P, puslaidininkių fizika – P 265)

Nariai:

prof. habil. dr. Gytis Juška (Vilniaus universitetas, fiziniai mokslai, fizika – 02 P, puslaidininkių fizika – P 265)

prof. dr. Vytautas Kleiza (Kauno technologijos universitetas, fiziniai mokslai, informatika – 09 P, matematinė ir bendroji teorinė fizika, klasikinė mechanika, kvantinė mechanika, reliatyvizmas, gravitacija, statistinė fizika, termodinamika – P 190)

prof. habil. dr. Romualdas Navickas (Vilniaus Gedimino technikos universitetas, technologijos mokslai, elektros ir elektronikos inžinerija – 01 T), mikroelektronika – T 171)

prof. habil. dr. Antanas Feliksas Orliukas (Vilniaus universitetas, fiziniai mokslai, fizika – 02 P, puslaidininkių fizika – P 265)

Oponentai:

prof. habil. dr. Adolfas Dargys (Fizinių ir technologijos mokslų centro Puslaidininkių fizikos institutas, fiziniai mokslai, fizika – 02 P, puslaidininkių fizika – P 265)

prof. habil. dr. Eugenijus Šatkovskis (Vilniaus Gedimino technikos universitetas, fiziniai mokslai, fizika – 02 P, puslaidininkių fizika – P 265)

Disertacija bus ginama viešame Fizikos mokslo krypties tarybos posėdyje 2012 m. rugsėjo mėn. 13 d. 16.00 val. Fizinių ir technologijos mokslų centro Puslaidininkių fizikos instituto posėdžių salėje, A. Goštauto g. 11, LT–01108 Vilnius, Lietuva.

Disertacijos santrauka išsiuntinėta 2012 m. rugpjūčio mėn. 13 dieną.

Disertaciją galima peržiūrėti Fizinių ir technologijos mokslų centro ir Vilniaus universiteto bibliotekose.

Introduction

In everyday life we are encountering more and more with mobile phones, personal computers, photo cameras and other devices which production is highly automated and constantly has to fulfil strict requirements. In modern microelectronics silicon has become a prior component, since its properties are well analyzed and the technology itself is elaborated. However, recently other semiconductors are used along with the silicon. Their new properties allow us the development of new semiconductor devices, emitting diodes or solid state lasers. We can modify properties of the semiconductor devices by adjusting the settings of quantum structures. Also heterojunction – based field-effect transistors and microwave radiation sensors are currently created. For the microwave electric field enhancement and signal processing GaAs electronics uses field-effect transistors with Schottky barrier or with heterojunction structures.

Recently, it was observed that electron drift velocity under strong electric fields in the AlGaAs/GaAs quantum well heterostructure can significantly exceed the electron drift velocity observed in the bulk GaAs. [1–3]. This allows us to produce microwave field–effect transistors, which would operate within the 100 GHz frequency range by using only standard lithographic processes. Modulation-doped $In_{0.52}Al_{0.48}As/In_{0.53}Ga_{0.47}As/In_{0.52}Al_{0.48}As$ nanometric heterostructures with high electron mobility and drift velocity in the InGaAs quantum well are the main semiconductor structures for the production of field–effect transistors operate within 100 GHz frequency range. Recently, these heterostructures were considered as a suitable semiconductor that generators and detectors of the electromagnetic radiation in the THz frequency band [4–5]. Performance of the microwave sensor which operates in wide frequency range is based on the non-homogenous charge carrier heating of an asymmetrically shaped two-dimensional electron gas structure [6]. Power–voltage sensitivity of such microwave diodes depends on the electron mobility in a two-dimensional electron gas channel and it is tens of times higger than that of the bulk GaAs narrowed structures with n-n^{+} junctions at the liquid nitrogen temperatures.

Asymmetrical shape of semiconductor structures narrowed down to the submicrometric sizes allows to increase the sensitivity of the microwave sensor in the bulk material and in the two-dimensional material up to several hundred volts per watt at liquid nitrogen temperatures [7]. The experimental results of the asymmetrical shape

diodes with two-dimensional electron gas and with the partial gate over the two–dimensional electron gas channel are presented in this work. Moreover, the charge carrier saturation velocity and mobility measurement results are presented in the dissertation. These properties are important in the process of the increasing operating rates of field-effect transistors.

Object of the research

The objects of investigations are semiconductor AlGaAs/GaAs, AlGaAs/InGaAs/AlGaAs and InAlAs/InGaAs/InAlAs heterostructures used for microwave electronics.

Aim of the research

The aim of this research is to investigate electrical properties of the low-dimensional semiconductor heterojunctions in the microwave electric field, as well as to suggest ways to increase the sensitivity of microwave sensors and operating speeds of field-effect transistors using peculiarities of electrical properties of low-dimensional semiconductor heterojunctions.

Main tasks of the work

- To investigate interaction of microwave electric field with semiconductor AlGaAs/GaAs and AlGaAs/InGaAs/AlGaAs nanostructures
- To measure current–voltage characteristics of semiconductor AlGaAs/GaAs, AlGaAs/InGaAs/AlGaAs and InAlAs/InGaAs/InAlAs nanostructures in high electric fields.
- To determine electron drift velocity and mobility dependence on electric field strength in semiconductor AlGaAs/GaAs, AlGaAs/InGaAs/AlGaAs and InAlAs/InGaAs/InAlAs nanostructures.
- To investigate possibilities (and conditions) for the increase of the electron drift velocity in the semiconductor AlGaAs/GaAs, AlGaAs/InGaAs/AlGaAs, InAlAs/InGaAs/InAlAs quantum wells in strong electric fields.

Research methods

Electrical properties of low dimension heterojunction semiconductor structures were investigated using two methods: by electron heating in strong microwave electric field and in strong direct current electric field.

Scientific novelty

It is established experimentally that electron drift velocities in the heterojunction InAlAs/InGaAs/InAlAs structures can reach 5×10^7 cm/s value; in the GaAs quantum wells 2D electron drift velocity can reach the value up to 1.6×10^7 cm/s.

There was determined that electron scattering can be confined by the insertion of phonon walls into the heterojunction quantum well. This approach allows us to obtain higher electron drift velocities.

Practical value of the scientific work

Results of this scientific work may be used to develop sensitive microwave detectors and to increase the operating speeds of the high speed two-dimensional field–effect transistor. Asymmetrically shaped microwave diodes made of AlGaAs/GaAs and AlGaAs/InGaAs/AlGaAs structures have greater sensitivity than the diodes made from bulk GaAs.

Statements to defend

- The gate–like metallization over the active layer of asymmetrically shaped modulation-doped AlGaAs/GaAs microwave diode increases the sensitivity of the diodes by three orders.
- In the AlGaAs/GaAs/AlGaAs nanostructure quantum well with the δ-doping, the electron drift velocity saturation value is 1.6 times higher than in the bulk GaAs due to reduced charge carrier scattering on optical and intervalley phonons.
- The insertion of thin layers of InAs (phonon walls) into AlGaAs/GaAs/AlGaAs and InAlAs/InGaAs/InAlAs quantum well nanostructures decreases the electron scattering on optical phonons and increases the saturated electron drift velocity values up to 2.1×10^7 cm/s and 5×10^7 cm/s values, respectively.

Approval of the research results

The main results were published in five papers (*Acta Physica Polonica A, Lithuanian Journal of Physics, Semiconductors – Физика и Техника Полупроводников*) and were presented at 6 conferences, 5 of them were international. The chronological order of the presentations made at the conferences is: *An International Joint Conference of 4th ESA Workshop on Millimetre Wave Technology and Applications* (Finland, Espoo – 2006), *XXXV International School on the Physics of Semiconducting Compounds* (Poland, Jaszowiec – 2006), *10-th Annual Directed Energy Symposium* (USA, Alabama, Huntsville – 2007), *38-th Lithuanian National Physics Conference* (Lithuania, Vilnius – 2009), *30-th International Conference on the Physics of Semiconductors* (South Korea, Seul, COEX – 2010), *14-th International Symposium on Ultrafast Phenomena in Semiconductors* (Lithuania, Vilnius – 2010 – 2 reports).

Structure of the dissertation

The dissertation consists of introduction, review of literature, description of the experimental methods and sample preparation and analysis of the results, summary of the work, list of references and list of author's publications. The dissertation contains 7 tables, 60 figures and graphs. The total volume of the work is 112 pages.

"Introduction"

The motivation, the objects and aim of research, main tasks, scientific novelty, practical analysis and statements for defence are presented in the Introduction.

Chapter 1. "Literature review"

In this part of the dissertation the hot charge carrier created electromotive force generation and measurment techniques (contact and contactless) will be presented.

Moreover, theoretical equations of asymetrically shaped microwave diodes are presented in this chapter. There are also brief description of heterojunction semiconductor structures, their properties and application in the semiconductor devices.

Chapter 2. “Methodology for investigation”

This chapter provides research methodology, which was used in this work. Furthemore, methods of heating charge carriers are described: using direct current voltage pulses and strong microwave electric field technique. Scheme of strong electric field equipment for the investigation of the heterojunction structure is given below (Fig. 1)

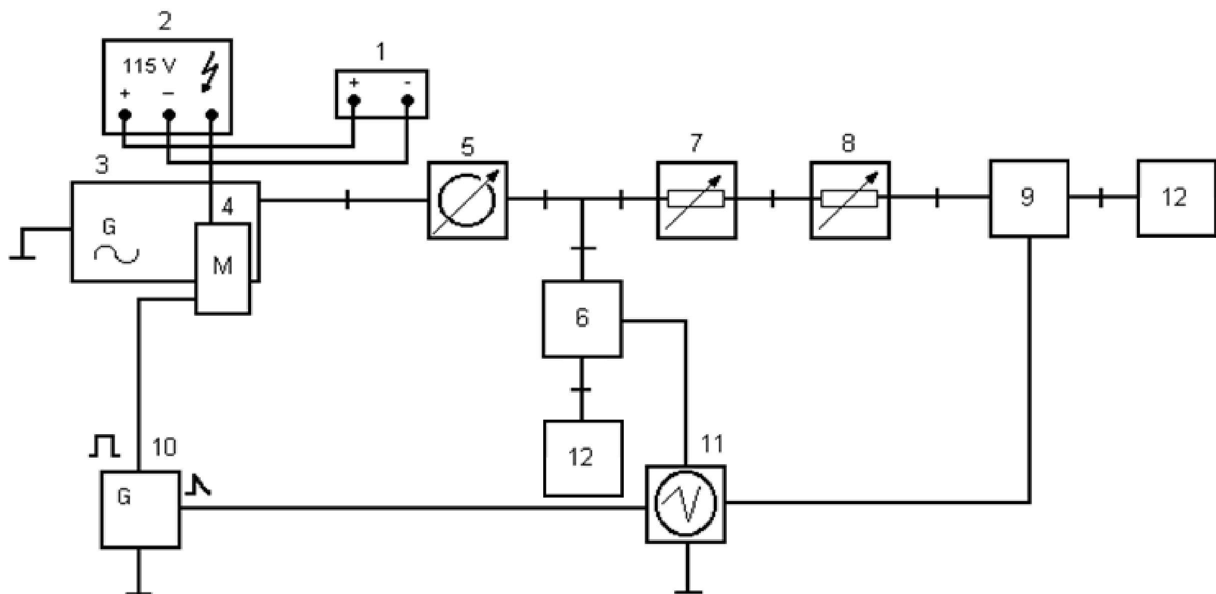

Fig. 1. Schematic illustration of microwave measuring of sample parameters in the high electric fields at 8 – 12 GHz frequency range: 1 – energy source, 2 – 115V 400 Hz energy source, 3 – high-power magnetron generator, 4 – electrical switch (commutator), 5 – valve; 6 –control head of the detector, 7, 8 – suppressors; 9 – wave emitting head with probe, 10 – pulse generator, 11 – oscillograph, 12 – harmonized loads.

Also the current-voltage measuring characteristics equipment which as used to measure the electron drift velocity of the charge manually and using automated processes is described. Automated system of measuring current-voltage characteristic is shown below (Fig. 2)

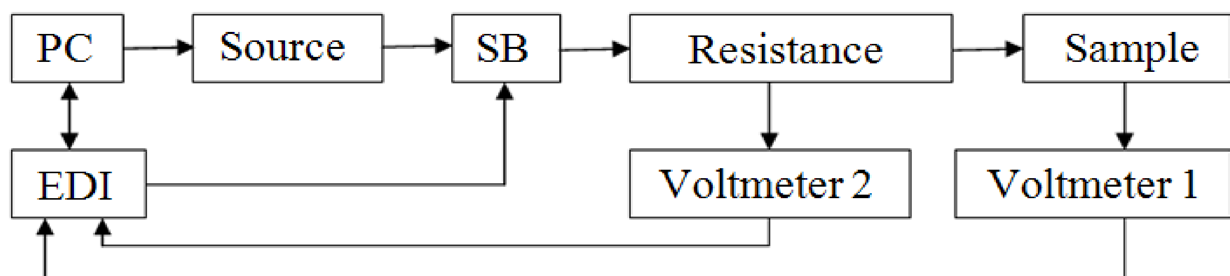

Fig. 2. Schematic illustration of automated system for measuring current-voltage characteristics. Notations of schematic illustration: PC – personal computer, source – voltage source, SB – switch box, resistance, sample, voltmeter 1 and voltmeter 2 and EDI – electronic devices interface. Taken from [8].

Chapter 3. “Asymmetrically shaped AlGaAs/GaAs microwave diodes”

In this part of the dissertation semiconductor samples: $Al_{0.25}Ga_{0.75}As$ and $Al_{0.28}Ga_{0.72}As/In_{0.15}Ga_{0.85}As/GaAs$ had been investigated. Heterojunction structures had been grown according to contract Nr. RITA–2003–506095 and Nr. HRPI–CT–2001–00114 at the Braun Submicron Research Center as well as in Institute of Microwave electronics of Russian Academy Sciences. The $Al_{0.28}Ga_{0.72}As/In_{0.15}Ga_{0.85}As/GaAs$ quantum well structures were grown in Cephona Centre of Excellence (Warsaw).

“Crystal“ microwave diodes were used in the research, and were made of layers grown on the Substrate. Scheme (Fig. 3) below shows us an example of the “crystal“ microwave diode. Dimensions of the diode are in hundreds of micrometres range. Microwave diode active area has a form of asymmetrical shaped semiconductor.

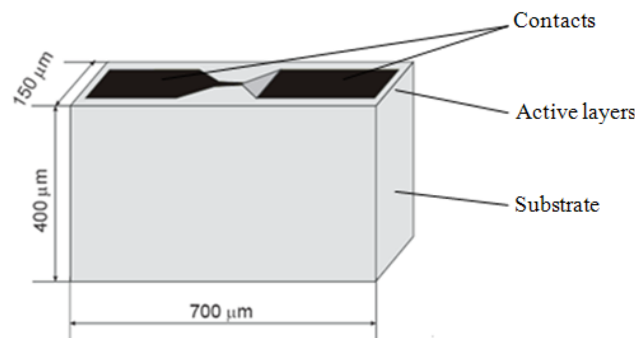

Fig. 3. Microwave diode, made on crystal basis.

For production of the microwave diodes there were used modulation-doped semiconductors AlGaAs/GaAs and $Al_{0.28}Ga_{0.72}As/In_{0.15}Ga_{0.85}As/GaAs$ heterostructures. MBE method was used for growing material of the semiconductor. Two types of layers were grown: with homogenous doped $Al_{0.25}Ga_{0.75}As/GaAs$ heterostructures as well as with δ–doped barrier in the $Al_{0.28}Ga_{0.72}As/In_{0.15}Ga_{0.85}As/GaAs$ heterostructures. Asymmetrical formation of meza was obtained by using chemical etching technology. Etching was made a little bit deeper than non doped n^+–$Al_{0.28}Ga_{0.72}As$ layer. The horizontal width of the narrowest asymmetrically shaped structure of the microwave diode is up to 7 µm. Second photolitographical process was used in the formation of metal contacts.

Properties of the asymmetrically narrowed structure were examined in the paper [8M], which had shown that: semiconductor structure sensitivity is proportional to the charge carrier mobility. The paper analyzed several semiconductor-based microwave diodes without gate and microwave diode with gate voltage sensitivity properties. Fig. 4 shows photos of the: a) of the symmetrical microwave diode, b) of the asymmetrically

shaped microwave diode, and c) of the asymmetricaly shaped microwave diode with gate. Samples were placed in a rectangular waveguide holder which was later mounted in the waveguide track. Measurements were performed using 10 GHz magnetron pulse modulated radiation. Pulse duration was 1.5 μs and the repetition rate of the pulses was 35 Hz.

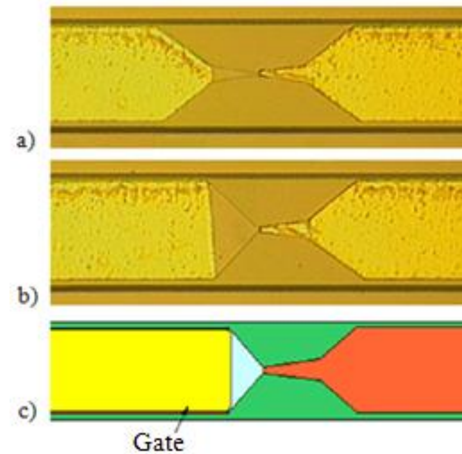

Fig. 4. Symmetrical form of a microwave diode a) and asymmetrical form of a microwave diode b) photos and asymmetrical form of the microwave diode with gate c)

During the research it was observed that the different microwave diode detection characteristics which were measured in the microwave electric field were quantitively different. One of the most significant voltage sensitivity differences was observed while analyzing different structures of microwave diodes at room temperature and at liquid nitrogen temperature. In Fig. 5 and Fig. 6 we can see the detected voltage dependence on the electric field of microwave power, when the diode had gate (round points) and with absence of it (square points) [6M]. Voltage–power characteristics measurements of the diodes were obtained at 10 GHz frequency. Microwave diode voltage–power sensitivity at the room temperature reached approximately $S_R = 0.3$ V/W value, when for the microwave diodes with gate the voltage–power sensitivity was significantly higher and reached $S_R = 3$ kV/W value (Fig. 5). Testing the same diodes in the liquid nitrogen temperature, gave as a result of bigger voltage–power sensitivity: microwave diodes without gating – $S_N = 25$ V/W, and microwave diodes with gating – $S_N = 100$ kV/W (Fig. 6).

We should notice that: voltage–power sensitivity of the microwave diode with gate at room temperature is two times bigger comparing with the microwave diode without gate at liquid nitrogen temperature. Therefore, it can be claimed that such a high sensitivity of the voltage–power characteristics in the microwave diodes can be used to detect nanowatt orders of the microwave power signals at room temperature. Previously mentioned, dynamic range of the diode varies over a wide microwave power range and depends on voltage–power sensitivity. From Fig. 5 and Fig. 6 we can see that at room temperature; microwave diode without gate voltage–power sensitivity linearly depends on microwave field power in 2 mW – 150 mW power range. Dynamic range of

microwave diode with gate is limited by 1 μW – 0.2 mW range. At liquid nitrogen temperature, microwave diode without gate voltage–power dependence is almost linear in the range from 0.02 mW up to 40 mW microwave power range. Microwave diode with gate has the linear voltage–power dependence in the 20 nW – 1 μW microwave power range [6M].

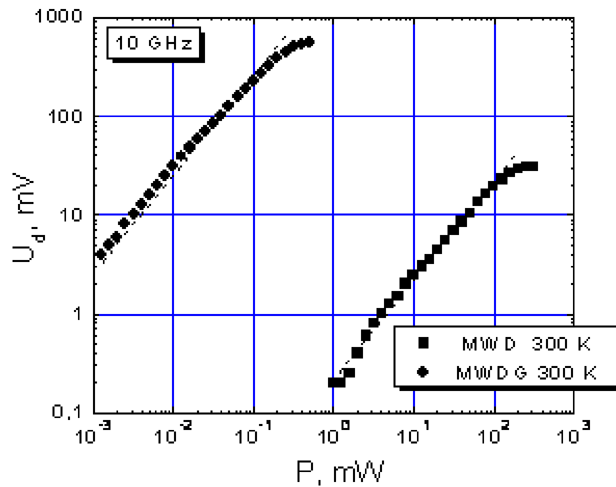

Fig. 5. Microwave diodes without gate (square points) and with gating (round points) voltage–power sensitivity characteristics at the room temperature.

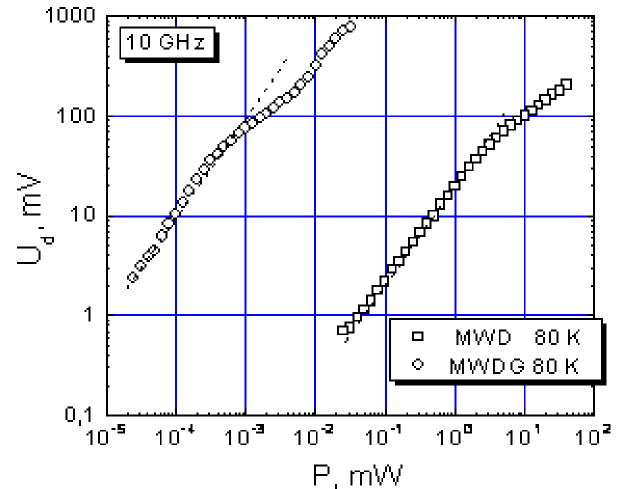

Fig. 6. Microwave diodes without gate (square points), and with gating (round points) voltage–power sensitivity characteristics at liquid nitrogen.

Further, the voltage–power characteristic of the microwave diodes with gate was analyzed. Obtained results can lead us to conclusion that the voltage–power sensitivity of the microwave diode at room temperature is inversely proportional to the size of the narrowest part of the diode. It means that sensitivity is $S_R = 400$ V/W at 1 μm width, $S_R = 250$ V/W at 2 μm width and $S_R = 180$ V/W at 3 μm width. However, at liquid nitrogen temperature the peak of the voltage–power sensitivity, which reached $S_N = 350$ kV/W, was typical for the microwave diodes which had the widest narrowing. From these results we can state that asymmetrically shaped microwave diodes with gate are suitable for the detection of low power the electromagnetical radiation [6M].

During the experiment voltage–power sensitivity of the modulation-doped $Al_{0.28}Ga_{0.72}As/In_{0.15}Ga_{0.85}As/GaAs$ structure, which had one $In_{0.15}Ga_{0.85}As$ channel, was analyzed. It gave us the results that at the 10 GHz frequency, the dependence of the detected voltage on the power was linear when the microwave electric field radiation was low. Reducing the samples temperature the voltage–power sensitivity of the diode

increased. It means that if at room temperature sensitivity was approximately $S_R \approx 0.6$ V/W, at the liquid nitrogen temperature it will increase up to the $S_N \approx 40$ V/W. It gave us a result that lowering temperature from room to liquid nitrogen, microwave diode voltage–power sensitivity had increased more than 60 times [5, 8M].

From the measurement results it can be suggested that modulation-doped $Al_{0.28}Ga_{0.72}As/In_{0.15}Ga_{0.85}As/GaAs$ heterostructure is more sensitive to the microwave power at liquid nitrogen temperature comparing to the sensitivity of moduliation-doped $Al_{0.25}Ga_{0.75}As/GaAs$ heterojunction. Sensitivity of the modulation-doped $Al_{0.28}Ga_{0.72}As/In_{0.15}Ga_{0.85}As/GaAs$ heterostructural microwave diode is about one and the half times higher compared to the modulation-doped $Al_{0.25}Ga_{0.75}As/GaAs$ samples.

To conclude, we can state that using charge-carrier heating method in microwave electric field will gives us following results:

Asymmetrically shaped modulation-doped microwave diode made of $Al_{0.25}Ga_{0.75}As/GaAs$ heterostructure with partial metallic gate has the high voltage–power sensitivity – $S_R = 200$ V/W at room temperatures, and at liquid nitrogen temperature it can reach about $S_N = 300$ kV/W. It was also found that the sensitivity is 3 orders bigger than the $Al_{0.25}Ga_{0.75}As/GaAs$ heterostructural microwave diode without partial metallic gate.

Experimentally it was found that $Al_{0.28}Ga_{0.72}As/In_{0.15}Ga_{0.85}As/GaAs$ heterostructural microwave diodes voltage–power sensitivity is twice bigger than $Al_{0.25}Ga_{0.75}As/GaAs$.

Chapter 4. "2–DE drift velocity in the InAlAs/InGaAs/InAlAs, AlGaAs/GaAs/AlGaAs and AlGaAs/GaAs heterostructure quantum wells"

For deeper understanding of voltage–power characteristics it was decided to investigate current–voltage characteristics of semiconductor structure, in order to improve the voltage–power sensitivity characteristics of microwave diodes and field effect transistors. We already know, that the sensitivity would increase, if carrier mobility was increased as well. Analysis of the investigated semiconductor current–

voltage material properties, the charge carrier drift velocity helps us to determine the frequency characteristics of diodes and field effect transistors.

Samples

A series of samples with different configurations of $In_{0.53}Ga_{0.47}As$ QW and differently located InAs spacers in it were grown to study the effect of introduction of InAs phonon walls on the electron mobility and drift velocity in the QW in strong electric fields [3M].

The structures grown by molecular beam epitaxy are shown schematically in Table 1. Three pairs of $In_{0.52}Al_{0.48}As/In_{0.53}Ga_{0.47}As/In_{0.52}Al_{0.48}As$ heterojunction with 16 and 17 nm thick InGaAs QWs were grown. Two samples were uniform QWs silicon doped from two sides (sample 794) or one side (sample 802). The other samples contained corresponding structures with thin (12 or 35 Å) InAs spacers in the QW, with the same QW thickness. One InAs spacer was introduced into the QW center in structure 796, while structures 803 and 805 contained two InAs spacers arranged symmetrically with respect to the QW center. Samples 804 and 805 contained additional GaAs spacers (1.1 nm) in the InGaAs/InAlAs junctions of the QW, which served as the phonon walls. The thicknesses of the GaAs and InAs spacers were chosen so as to ensure two-dimensional growth of these layers without lattice relaxation defects and to reduce to a minimum the effect of these layers on the energy band structure. The experimentally determined Hall mobility μ_H and carrier concentration N_{s0} in the heterostructures are listed in Table 2.

Also we studied eight types of heterostructures, whose parameters are listed in the Table3. Structure 4T is the single-junction $Al_{0.25}Ga_{0.75}As/GaAs$ heterostructure with the δ-doped (with Si) barrier and the triangular QW with the effective width at the level of the lower electron state $z_0 = 6$ nm. Structures 660 and 17π are the two-barrier $Al_{0.3}Ga_{0.7}As/GaAs/Al_{0..3}Ga_{0.7}As$ heterostructures with the δ-doped (Si) barriers on both sides; structures 660 and 17π differ in QW width: the QW widths are 10 nm in structure 660 and 26 nm in structure 17π. Structure 663 is the pseudomorphous two-barrier $Al_{0.36}Ga_{0.64}As/In_{0.15}Ga_{0.85}As/Al_{0.36}Ga_{0.64}As$ heterostructure with the heavily doped $In_{0.15}Ga_{0.85}As$ layer. To study the current–voltage (*I*–*U*) characteristics of channels in the heterostructures, we fabricated the samples of gateless mesa structures with the width

100μm. The Au/Ni/Ge ohmic contacts were 100×100 μm in area. The distance between the source and drain contacts *d* was varied from 6 to 90 μm [4M].

Table 1. The layer compositions of $In_{0.52}Al_{0.48}As/In_{0.53}Ga_{0.47}As/In_{0.52}Al_{0.48}As$ heterojunction samples. The thicknesses of the InP substrate and only $In_{0.52}Al_{0.48}As$ buffer (in μm) and other layers (in nm).

<table>
<tr><td>Sample no.</td><td>794</td><td>796</td><td>802</td><td>803</td><td>804</td><td>805</td></tr>
<tr><td>top $In_{0.53}Ga_{0.47}As$ layer</td><td>6</td><td>6</td><td>6</td><td>6</td><td>6.1</td><td>6.1</td></tr>
<tr><td>$In_{0.52}Ga_{0.48}As$ barrier</td><td>17</td><td>17</td><td>30</td><td>30</td><td>28.1</td><td>28.1</td></tr>
<tr><td>δ – Si</td><td>+</td><td>+</td><td>+</td><td>+</td><td>+</td><td>+</td></tr>
<tr><td>spacer $In_{0.52}Ga_{0.48}As$ layer</td><td>4.5</td><td>4.5</td><td>6.5</td><td>6.5</td><td>6</td><td>6</td></tr>
<tr><td rowspan="7">$In_{0.53}Ga_{0.47}As$ channel</td><td rowspan="7">17</td><td rowspan="3">6.75</td><td rowspan="7">16</td><td rowspan="2">4.5</td><td>GaAs 1.1</td><td>GaAs 1.1</td></tr>
<tr><td rowspan="5">13.8</td><td>3.47</td></tr>
<tr><td>InAs 1.2</td><td>InAs 1.2</td></tr>
<tr><td>InAs 3.5</td><td>4.5</td><td>4.5</td></tr>
<tr><td rowspan="3">6.75</td><td>InAs 1.2</td><td>InAs 1.2</td></tr>
<tr><td rowspan="2">4.5</td><td>3.47</td></tr>
<tr><td>GaAs 1.1</td><td>GaAs 1.1</td></tr>
<tr><td>spacer $In_{0.52}Ga_{0.48}As$ sluoksnis</td><td>4.5</td><td>4.5</td><td>-</td><td>-</td><td>-</td><td>-</td></tr>
<tr><td>δ – Si</td><td>+</td><td>+</td><td>-</td><td>-</td><td>-</td><td>-</td></tr>
<tr><td>$In_{0.52}Ga_{0.48}As$ buffer layer, μm</td><td>0.24</td><td>0.24</td><td>0.24</td><td>0.24</td><td>0.24</td><td>0.24</td></tr>
<tr><td>InP substrate, μm</td><td>400</td><td>400</td><td>400</td><td>400</td><td>400</td><td>400</td></tr>
</table>

Table 2. Sheet electron density N_{s0}, carrier mobility μ_H of the Hall measurements [4M]

Sample no.	794	796	802	803	804	805	29B
N_{s0}, 10^{12}cm^{-2}	3.5	2.5	1.3	1.3	1	1.2	1.4
μ_H, 10^3cm^2/(V·s)	10.2	12.3	11.7	11.4	9.9	8.4	12.3

Table 3. The main parameters of the experimentally investigated samples.
* The effective QW width z_0 at the level of the lowest electronstate is given.
B** with InAs barriers in the GaAs QW
T*** the single heterojunction $Al_{0.3}Ga_{0.7}As/GaAs$ modulation-doped structure (triangular QW)
**** Width of the lowest subband inversion layer

Structure type	QW width *L*, nm	Concentration of electrons N_s, 10^{12}cm^{-2}
4T ($Al_{0.25}Ga_{0.75}As/GaAs$)	6*	1.2
660 ($Al_{0.3}Ga_{0.7}As/GaAs/Al_{0.3}Ga_{0.7}As$)	10	1.0
17π ($Al_{0.3}Ga_{0.7}As/GaAs/Al_{0.3}Ga_{0.7}As$)	26	0.7
663 ($Al_{0.36}Ga_{0.64}As/In_{0.15}Ga_{0.85}As/Al_{0.36}Ga_{0.64}As$)	16	6
A($Al_{0.3}Ga_{0.7}As/GaAs/Al_{0.3}Ga_{0.7}As$)	30	0.8
B** ($Al_{0.3}Ga_{0.7}As/GaAs/Al_{0.3}Ga_{0.7}As$)	30	0.6
C ($Al_{0.3}Ga_{0.7}As/GaAs/Al_{0.3}Ga_{0.7}As$)	10	1.25
T*** ($Al_{0.3}Ga_{0.7}As/GaAs$)	6****	2.6

The experimental measurements of the electron drift velocity at high electric fields in the $Al_{0.3}Ga_{0.7}As/GaAs/Al_{0.3}Ga_{0.7}As$ structures with different widths L_z of the GaAs QW were performed [2M]. Table 1 shows the parameters of the investigated structures. All samples have 100×100 μm^2 ohmic contacts (Au/Ni/Ge) with different spacing d between them (from 10 to 100 μm). Schematic view of samples is presented in the Fig. 7.

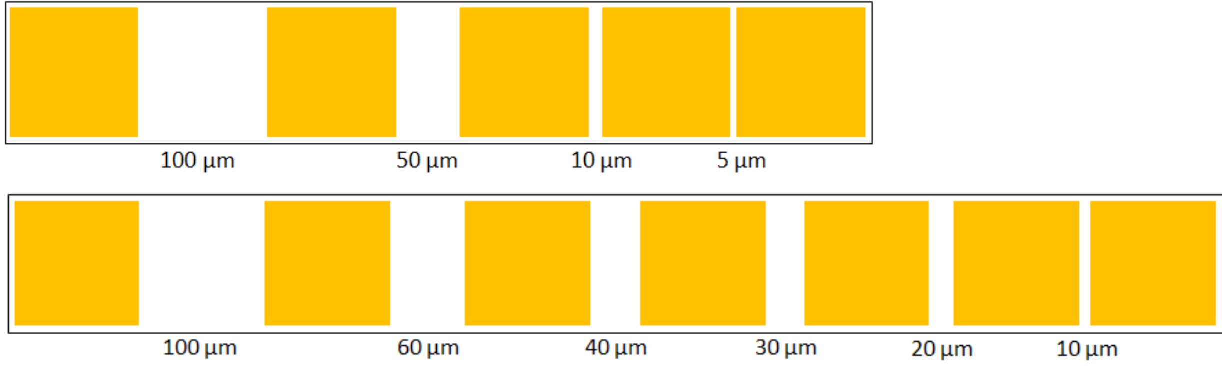

Fig. 7. Schematic view of samples for current–voltage characteristics measuring (marked in dark (100×100µm) contacts, the numbers mark the distance between contacts).

Change in electron density and mobility in InGaAs QWs at low electric fields

Electron transport in the $In_{0.53}Ga_{0.47}As/In_{0.52}Al_{0.48}As$ heterostructures of five types with a quantum well (QW) width of 16 nm was investigated. Structures 805 and 796 are with inserted thin (1–2 nm) InAs layers and have higher mobility in comparison with structures 804 and 794 without the InAs spacers. The thin electron transparent InAs spacer is assumed to be reflecting for optical phonons and is considered as a phonon barrier or phonon wall.

The highest mobility has structure 29B with the increased InAs component in the $In_{0.8}Ga_{0.2}As/In_{0.7}Al_{0.3}As$ heterostructures. Fig. 8 shows the dependences of current I along the InAlAs/InGaAs/InAlAs QW layer with modulation-doped InAlAs barriers on mean electric field strength $E = U/d$, where U is the applied voltage, in the samples with different source-drain lengths $d = 10$ and 100 μm. The widths of the mesastructure and ohmic contact (Au/Ni/Ge) are 100 µm [1M].

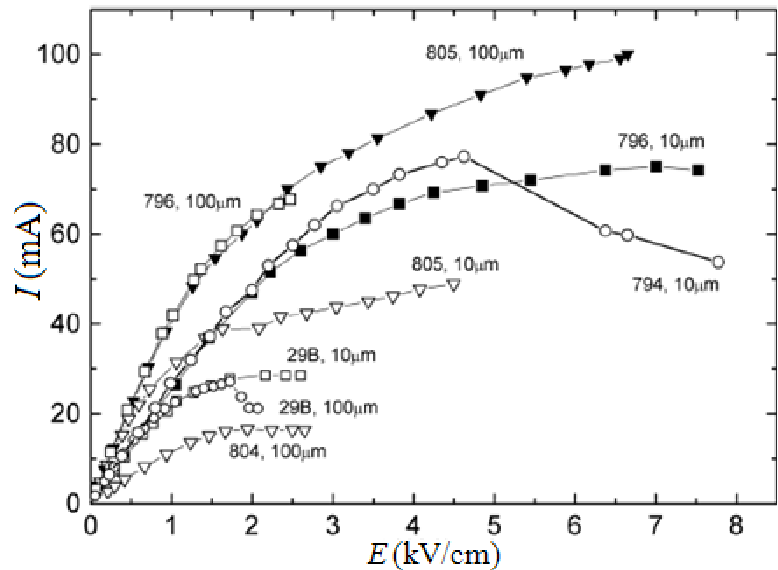

Fig. 8. Field dependences of the current along the InAlAs/InGaAs/InAlAs quantum well for different samples with source-drain lengths of 10 and 100 µm [1M].

To separate the contributions of changes in electron mobility and electron density to the current dependence on electric fields, the mobility was determined from magnetoresistance measurements in short (10 µm) samples. Fig. 9 shows the field dependences of the mobility in the investigated structures. One can see that at the fields E of 0–4 kV/cm, the mobility in samples 796 and 805 with the inserted InAs barriers, as well as in the samples with the increased InAs content in the modulation-doped heterostructure are larger than that in the structures without the InAs barriers. At fields $E<0.5$ kV/cm, the mobility in sample 29B is 1.7 times larger than in samples 794 and 804 without the barriers. The mobility in sample 805 with two inserted InAs barriers, and in sample 796 with the single InAs barrier is 1.4 and 1.1 times larger than in sample 794 and 804 without the barriers, respectively. The large mobility increase coincides with the calculated decrease of interface (IF) phonon scattering rate in the InAlAs/InGaAs structures [3M, 4M].

A large decrease in the mobility with increase of electric fields in the range of 0.5–4 kV/cm is observed. This is a specific property of modulation-doped heterostructures. In these structures, electron scattering by IF phonons is the predominant scattering mechanism. The increase of electron–IF phonon scattering rate by one order, when the electron energy exceeds the IF phonon energy (40–50 meV), is responsible for such strong mobility decrease in relatively low electric fields. Let us note that the decrease in the mobility is responsible for the increase in the threshold electric field for the intervalley transfer of electrons, E_{th}, which becomes larger than that in bulk InGaAs semiconductors. The electron density in the QW channel of the modulation-doped structure is determined by the potential difference between the ionized donor layer and the QW electron channel. This potential difference depends not

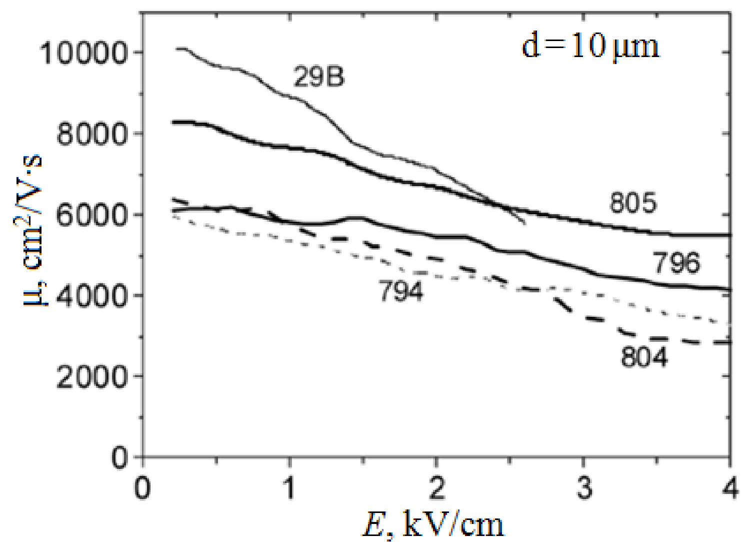

Fig. 9. Field dependence of the electron mobility in different samples. Solid and dashed lines represent the structures with the InAs spacers and without the spacers, respectively [1M].

only on the applied voltage U_D, but mostly on the preparation technology of the samples for measurements. The local disturbance of potential during preparation of ohmic contacts increases the electron density in the QW channel. In considered samples, this increase in the electron density $N_s(0.5)$ determined from magnetoresistance measurements at low electric fields, $E = 0.5$ kV/cm [1M].

Drift velocity of electrons in the AlGaAs/GaAs QW

To determine the specific features of the field dependence of the drift velocity of electrons in the QW, we experimentally studied the *I–U* characteristics of three types of $Al_{0.25}Ga_{0.75}As/GaAs$ and $Al_{0.3}Ga_{0.7}As/GaAs/Al_{0.3}Ga_{0.7}As$ structures: 4T, 660, and 17π (see table 3). Fig. 10 shows the field dependence of the current, $I(E)$, in the GaAs channel of structure A with the single AlGaAs/GaAs heterobarrier (triangular QW). The field in the sample is defined as $E = U/d$, where U is the voltage across the sample of length d. It is noteworthy that, for all of the five samples of structure A with different spacing d between the contacts, we obtained exactly the same results for the field dependence of the current. The field dependence of the current $I(E)$ completely defines the field dependence of the drift veliocity $v_{dr}(E) = I(E)/qN_s w$, where $w = 100$ μm is the channel width and q is the elementary charge. For structure A, the saturation of the current at 30 mA corresponds to the drift velocity $v_{sat} = 1.5\times10^7$ cm/s [4M].

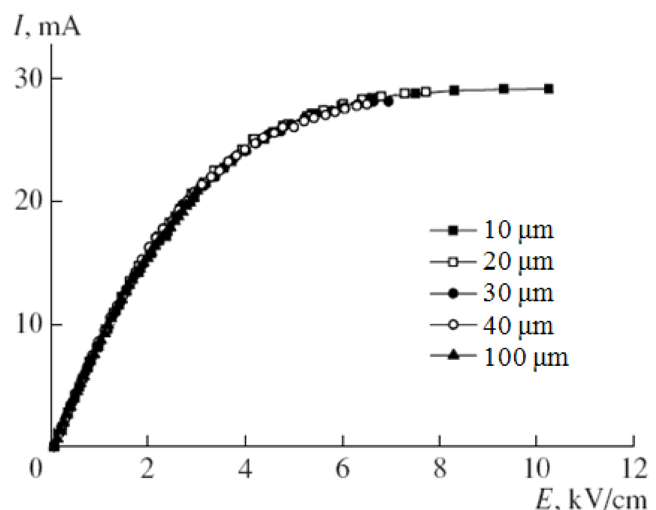

Fig. 10. The dependence of the current I on the electric field E in the QW of the single $Al_{0.25}Ga_{0.75}As/GaAs$ heterojunction (structure A) for the samples with the channel length $d = 10$, 20, 30, 40, and 100 μm. [4M].

There isn't negative differential conductivity in the field dependence of the mobility, and the electric field of 8 kV/cm, in which we observe saturation of the current, is noticeably higher than the threshold field 3 kV/cm of the *Γ–L* intervalley electronic transition responsible for a decrease in the drift velocity in bulk GaAs.

We attribute the experimentally observed sublinear dependence $v_{dr}(E)$ to the decrease in the rate of scattering of charge carriers in the upper *L* valleys of GaAs, when the electrons are captured by the triangular QW. When captured into the QW, the electrons in the upper valleys of GaAs increase their mobility. Therefore, the *Γ*–*L* intervalley transition in the fields 2–4 kV/cm does not result in the negative differential conductivity. Saturation of the drift velocity in high fields (8–12 kV/cm) is attributed to the electron transition from the *L* valley to the *X* valley [9]. The maximum drift velocity corresponding to saturation of the current in the GaAs QW of type A is 1.5 times higher than the saturation drift velocity 10^7 cm/s in bulk GaAs.

Fig. 11 shows the field dependences of the drift velocity in the samples of structures 660 and 17π. We obtained these dependences, taking into account the estimated variations in the concentration of charge carriers with the length *d*. In sample 660 with the QW with the width of $L = 10$ nm, the drift velocity saturates in the field 4 kV/cm and does not exceed the saturation drift velocity $v_{sat} = 10^7$ cm/s in the bulk material. In sample 17π with a wide QW in the field 15 kV/cm, the maximum drift velocity is higher than the saturation drift velocity in bulk GaAs by the factor 1.2. In this case, the threshold field of saturation of the velocity is higher than 10 kV/cm. This result is consistent with the estimates reported in [10, 11].

The rate of scattering of electrons by optical phonons decreases as the QW width is increased. In the QW with the width $L = 10$ nm, this rate is comparable with the rate of scattering in the bulk material. In the wider QW ($L = 26$ nm), the rate of scattering of electrons at optical phonons is several times lower than that in the bulk material. Correspondingly, with a field increase, in sample 17π, the drift velocity increases to much larger values than those in sample 660. Saturation of the drift velocity occurs due to the intervalley transition of electrons. This is suggested by the slightly pronounced negative differential conductivity observed in fields higher than the threshold field E_{th}, at which the drift velocity is maximal. In sample B with the narrow QW, the increase in the drift mobility is limited by the transition of electrons from the *Γ* valley to the *L* valley, since the scattering of electrons of the *L* valley at optical phonons in the narrower QW is efficient, and the mobility of the electrons is low. In sample 17π with the wide QW, the transfer of electrons from the *Γ* valley to the *L* valley does not limit the increase in the drift velocity, since the scattering of electrons of the *L* valley by optical phonons in the

wide QW is inefficient, and the mobility of the electrons is high. Limitation of the drift velocity occurs in higher fields, in which the electrons are transferred from the *L* valley to the *X* valley [4M].

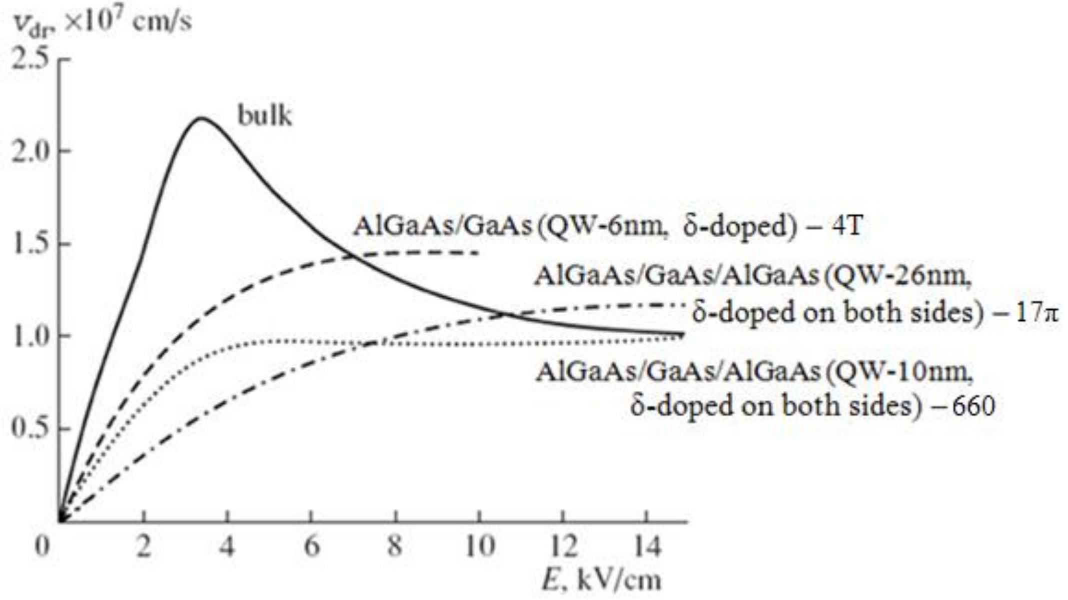

Fig. 11. Field dependences of the drift velocity of electrons $v_{dr}(E)$ in the GaAs QWs of the heterostructures of types 4T, 660, and 17π in comparison with the drift velocity in bulk GaAs [4M].

The experimental curves $v_{dr}(E)$ (Fig. 15) are adequately described by the expression [12]

$$v_{dr} = \frac{\mu E}{\sqrt{\left(1+\left(\frac{\mu E}{v_{sat}}\right)^2\right)}}, \tag{7}$$

where μ is the low-field electron mobility and v_{sat} is the saturation velocity. It is important that v_{sat} depends on the QW width: v_{sat} increases with an increase of QW width in accordance with the variations in the rate of scattering of electrons in the upper valleys of GaAs. It is worth noting that formula (1) is often used as an approximation in describing the characteristics of FETs [13, 14]. It is evident that, with the dependence of v_{sat} on the QW width, the above approximation is consistent with the real dependence $v_{dr}(E)$ for electrons in the QW [4M].

Drift velocity of electrons in the $Al_{0.36}Ga_{0.64}As/In_{0.15}Ga_{0.85}As$ structure

Fig. 12 shows the field dependence of the current of electrons in the channel of the double pseudomorphous $Al_{0.36}Ga_{0.64}As/In_{0.15}Ga_{0.85}As/Al_{0.36}Ga_{0.64}As$ heterostructure (type

663). Evidently, the dependence is sublinear and levels off in fields above 7 kV/cm. Due to the heavy doping of the $In_{0.15}Ga_{0.85}As$ channel directly, the conductivity layers parallel to the channel and the variations in the concentration of electrons in the channel with the sample length manifest themselves relatively slightly [4M].

It can be seen that, in the $In_{0.15}Ga_{0.85}As$ QW channel, the maximum velocity of electrons can reach 6×10^6 cm/s, which is nearly 1.3 times higher than the velocity in bulk $In_{0.15}Ga_{0.85}As$. In bulk $In_{0.15}Ga_{0.85}As$ with the low-field mobility $\mu = 1000$ cm^2(V s), the maximum drift velocity of electrons does not exceed 4.5×10^6 cm/s. Due to the substantially higher drift velocity in the QW, the pseudomorphous $Al_{0.36}Ga_{0.64}As/In_{0.15}Ga_{0.85}As/Al_{0.36}Ga_{0.64}As$ structure is successfully used in developing the microwave transistors [4M].

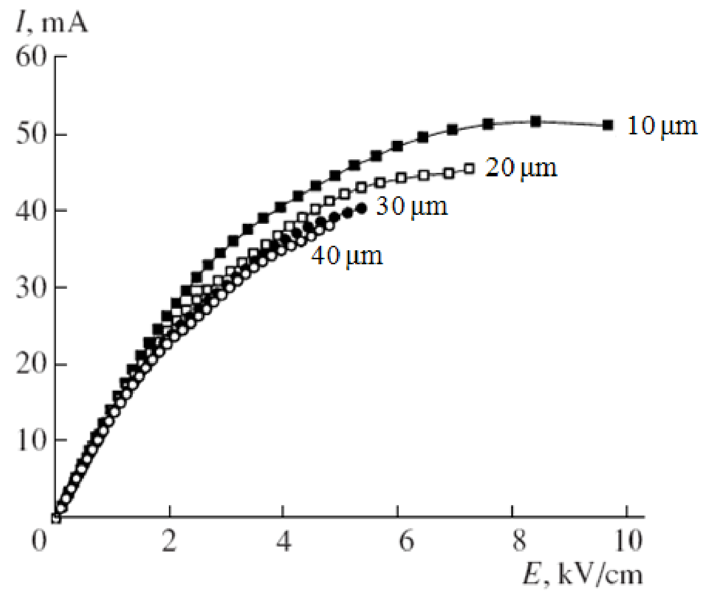

Fig. 12. Field dependences of the current in the $In_{0.15}Ga_{0.85}As/Al_{0.36}Ga_{0.64}As$ QW for the samples with the channel length d = 10, 20, 30, and 40 μm [4M].

The rate of electron scattering by polar optical and interface phonons in an $In_{0.52}Al_{0.48}As/In_{0.53}Ga_{0.47}As/In_{0.52}Al_{0.48}As$ QW with an InAs phonon wall

The thin electron-transparent InAs spacer is assumed to be reflecting for optical phonons, i.e., it is considered as a phonon wall. Some methods for calculating the electron scattering rate in QWs from localized interface and confined PO phonons were considered in [15, 16]. The dependences of the electron–phonon scattering rate in an $In_{0.52}Al_{0.48}As/In_{0.53}Ga_{0.47}As/In_{0.52}Al_{0.48}As$ QW without phonon walls on the electron energy, $W(E)$, calculated according to [15, 16] for the samples with QWs of different thickness, are shown in Fig. 13. The scattering rate from confined PO phonons, W_C, barely changes with change in the QW thickness in the range of 17–28 nm, whereas the scattering rate from the interface phonons of the QW external barriers, W_{IF}, decreases several-times. However, the scattering rate from the interface phonons of the external

barriers is always much higher than that for the confined PO phonons, W_C. The scattering from interface phonons is dominant in QWs thinner than 30 nm. The introduction of InAs phonon walls into the $In_{0.53}Ga_{0.47}As$ QW leads to localization of the confined PO phonons and the interface phonons of the InAs phonon wall in the narrower phonon wells (two walls in sample 796 and three walls in samples 803 and 805). The dependences of the scattering rate on the electron energy for the samples with InAs spacers are shown in Fig. 14. The dependence of the scattering rate from PO phonons for sample 794, which does not possess an InAs spacer (W_{C0}), is also shown for comparison. The dependences of the scattering rate on the electron energy, obtained with allowance for the scattering from confined PO phonons, W_{C1}, and for the scattering from interface phonons of the InAs spacers, W_{IF1}, are shown separately for samples 796 and 803. The introduction of thin InAs phonon walls reduces the electron scattering rate from the confined PO phonons by an order of magnitude. This decrease in the scattering rate is not compensated by the additional scattering from the interface phonons of the InAs spacers, W_{IF1}. In the QWs with InAs spacers, the total scattering rate by the PO phonons confined in the phonon wells and from the interface phonons of the InAs spacers, $W_{C1}+W_{IF1}$, is below the electron scattering rate from the PO phonons in QWs without InAs spacers, W_{C0}. [3M].

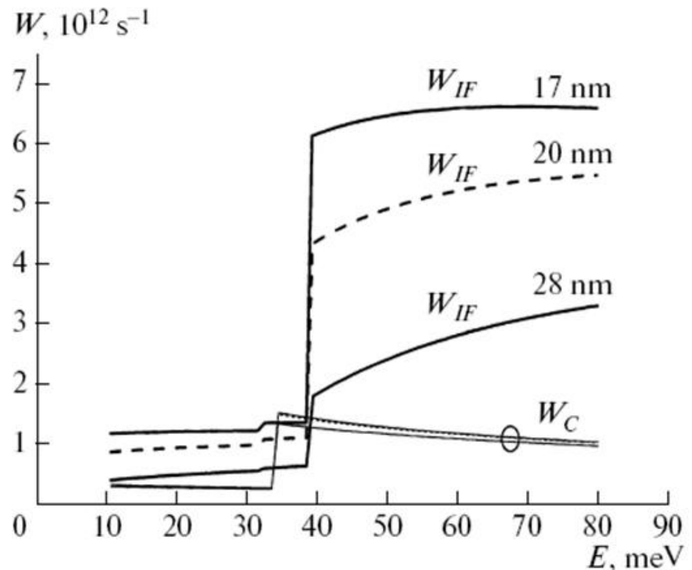

Fig. 13. Dependences of the scattering rate W due to the localized interface phonons (W_{IF}) and confined PO phonons (W_C) in the $In_{0.52}Al_{0.48}As/In_{0.53}Ga_{0.47}As/In_{0.52}Al_{0.48}As$ QWs with thicknesses of 17, 20, and 28 nm on the electron energy E [3M].

When one InAs spacer is introduced (sample 796), the scattering rate decreases by a factor of 2.8, whereas an introduction of two spacers (sample 803) leads to a decrease by a factor of 2.3 (Fig. 14). This means that an introduction of phonon walls into a QW reduces significantly the scattering rate and increases the electron mobility in the QW.

However, the InAs phonon wall is relatively transparent to the high energy IF phonons from the external $In_{0.52}Al_{0.48}As$ barriers. Its introduction into the QW does not change the scattering rate from the interface phonons of the external $In_{0.52}Al_{0.48}As$ barriers, W_{IF0}. Therefore, the ratio of the total scattering rate due to the PO and interface phonons in the absence of InAs spacers, $W_{C0} + W_{IF0}$, to the total scattering rate in the presence of barriers, $W_{C1} + W_{IF1} + W_{IF0}$, is only 1.23 for one InAs spacer introduced into the QW (sample 796) and 1.2 for two InAs spacers (sample 803) [3M].

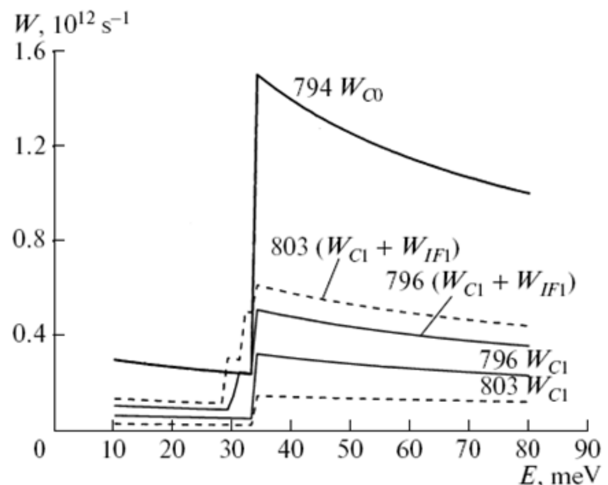

Fig. 14. Dependences of the scattering rate W from the interface phonons of InAs phonon barriers (W_{IF1}) and from the PO phonons confined between the InAs spacers (W_{C1}) on the electron energy E for samples 796 and 803. W_{C0} is the scattering rate due to the PO phonons in sample 794 without an InAs spacer [3M].

The low field electron mobility $\mu \approx 1/(W_{C1} + W_{IF1} + W_{IF0})$ increases by a factor of only 1.23 for samples 794 and 796 and by a factor of 1.2 for samples 802 and 803 after the insertion of InAs barriers. Thus, the scattering from the high–energy interface phonons of the external $In_{0.53}Ga_{0.47}As/In_{0.52}Al_{0.48}As$ barriers, which dominates over all other scattering channels, limits significantly the increase in the electron mobility as a result of the introduction of InAs spacers into the QW. Therefore, the search for ways to increase the mobility in InGaAs QWs by inserting phonon walls should be supplemented with a search for ways to control the scattering rate due to the interface phonons of the external QW barriers (InAlAs spacers) [3M].

The field dependences of the conduction in the $In_{0.52}Al_{0.48}As/In_{0.53}Ga_{0.47}As/In_{0.52}Al_{0.48}As$ QW were measured on the samples in the form of gateless mesa-structures 100 μm wide, with a deposited sequence of Au/Ni/Ge ohmic contacts having an area of 100×100 μm^2 and spaced by different distances: d = 5, 10,50, and 100 μm.

The field dependence of conductivity of the QW channel was determined from the measured dependences of the current through the channel, I_D, on the applied voltage U_{SD}. To prevent the samples from heating, the measurements were performed using voltage

pulses no longer than 1.2 μs with a repetition frequency of 100 Hz. The I_D–U_{SD} characteristics were found to depend on the contact resistances and intercontact length. The measurements of the complete series of I_D–U_{SD} characteristics with different gaps in each sample allow one to determine the contact resistances and, thus, the correct field magnitude. No significant increase in the mobility as a result of the introduction of InAs spacers into the InGaAs QW was observed for the sample pairs (802, 803) and (804, 805). However, the mobility in sample 796 with an InAs spacer at the QW center turned out to be higher than that in the barrierless sample 794 by a factor of 1.4, a value that even exceeds the theoretical decrease in the scattering rate due to PO phonons. We assume this rise in the mobility in sample 796 to be also due to the relatively large (3.5 nm) thickness of the InAs spacer and the effect of this barrier on the electron subsystem, as was observed in [17, 18]. Thus, it was confirmed experimentally that the confinement of PO phonons in the phonon well as a result of the InAs insertion into the QW may reduce the electron–phonon scattering and increase the electron mobility. However, the increase in the mobility is limited by the high scattering rate by the interface phonons of the QW lateral barriers [3M].

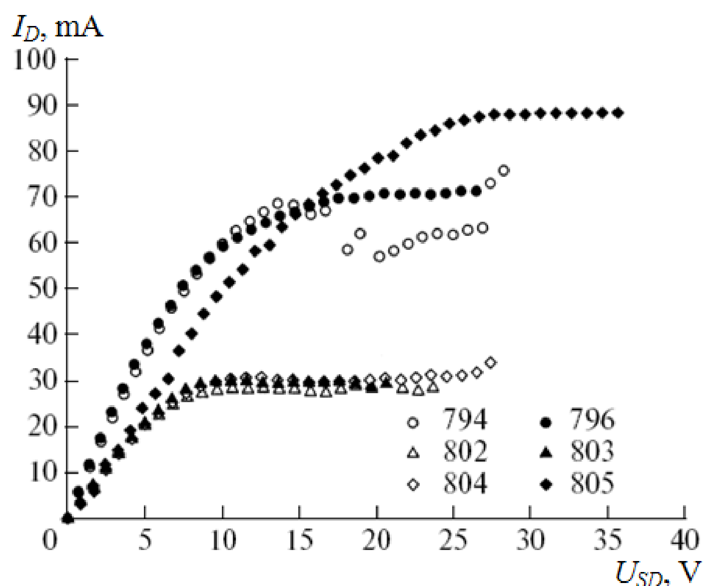

Fig. 15. Dependences of the current I_D along the QW channel on the applied voltage U_{SD} for three pairs of samples: 794/796, 802/803, and 804/805. The intercontact distance d = 50 μm [3M].

The I_D–U_{SD} characteristics in strong fields are sublinear dependences, with the current tending to a constant value; they are different for different samples (Fig. 15). On the assumption that the I_D–U_{SD} characteristics are determined by the field dependence of the drift velocity $v_{dr}(E)$ in InGaAs, we arrive at a conclusion that the dependences $v_{dr}(E)$ are quite different for different samples. The values of the saturation drift velocity v_{sat} in InGaAs and the critical field corresponding to the saturation in the InGaAs QW change several times from sample to sample. Therefore, the sublinear current–voltage dependences and the current saturation along the $In_{0.53}Ga_{0.47}As$ QW, which are observed

in our samples, cannot be explained by only the field dependence of the electron mobility. To explain these phenomena, one has to resort to an additional mechanism taking into account the change in the electron concentration in the QW channel with an increase in the voltage applied along the channel. A possible cause of the change in the electron concentration in the QW under a voltage applied along the QW channel is the charge induction in the QW with a change in the voltage between the two parallel channels, which form a δ-doped layer of positively charged donors in the InAlAs barrier and a negatively charged layer of electrons (charge carriers in the InGaAs QW) [3M].

The calculated dependences of the potential of the bottom of the conduction band in the $In_{0.52}Al_{0.48}As/In_{0.53}Ga_{0.47}As$ heterostructures with one- (sample 802) and two-sided δ-Si doping (thickness d_δ = 3 nm) of the InAlAs barrier (sample 794) are shown in Fig.

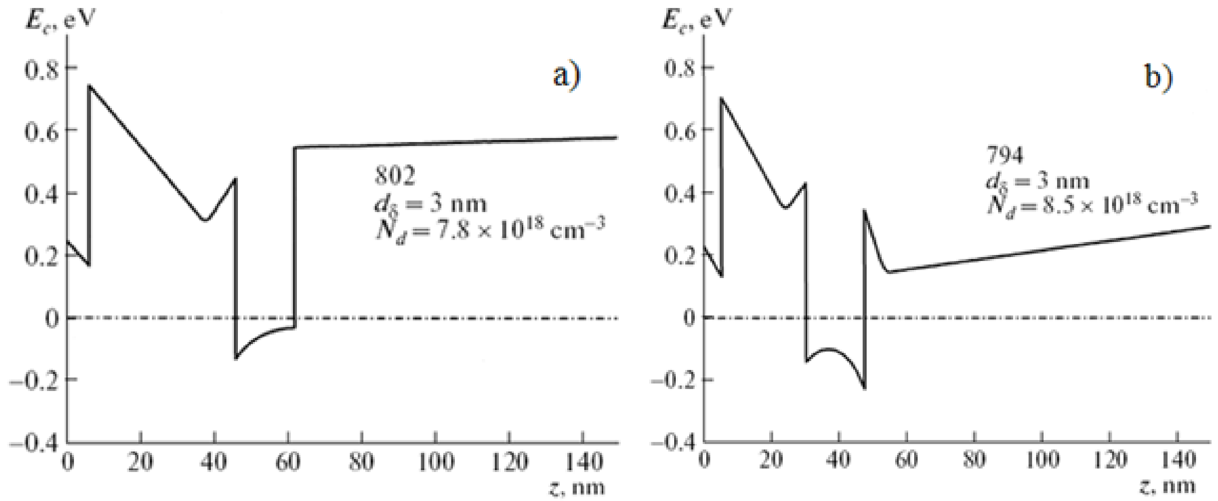

Fig. 16. Profiles of the conduction band $Ec(z)$ at 295 K in the $In_{0.52}Al_{0.48}As/In_{0.53}Ga_{0.47}As/In_{0.52}Al_{0.48}As$ heterostructures: (a) sample 802 with one sided δ-Si doping and (b) sample 794 with two sided δ-Si doping. The donor concentration N_d in the spacers is 7.8×10^{18} and 8.5×10^{18} cm^{-3}, respectively [3M].

16. One can see well the channels oriented parallel to the InGaAs QW: δ-doped layers in the InAlAs barriers, separated from the QW by 4.5 to 6.5 nm thick spacers. When a longitudinal (x coordinate) voltage U_{SD} is applied to the two parallel channels (QW and δ-doped layer), a transverse QW voltage U_{12} arises between the channels due to the difference in the distributions of the longitudinal (along the x coordinate) potentials in the QW, $\phi_1(x)$ and a second (parallel to the QW) channel, $\phi_2(x)$:

$$U_{12}(x) = \varphi_2(x) - \varphi_1(x). \quad (1)$$

The potential difference $U_{12}(x)$ between the channels determines the change in the induced electron concentration in the QW, ΔN:

$$q\Delta N(x) = C_{12} U_{12}(x), \qquad (2)$$

where q is the elementary charge and C_{12} is the capacitance between the channels, which is determined by the spacer thickness in the samples under study.

The relative change in the electron concentration in the QW is

$$\frac{\Delta N(x)}{N_{s0}} = \frac{U_{12}(x)}{U_T}, \qquad (3)$$

where U_T corresponds to the equilibrium electron concentration: $N_{s0} = (C_{12}/q)U_T$.

The current density in the cross section x of the QW channel, with assumption of the change in the electron concentration, is

$$j(x) = \sigma_0 \left(1 + \frac{U_{12}(x)}{U_T}\right) \frac{d\varphi_1(x)}{dx}. \qquad (4)$$

Correspondingly, the current through an InGaAs QW with a length d and a width w is

$$I_{san} = \frac{w}{d} \int_0^d j(x)dx. \qquad (5)$$

The model of electron induction in the QW in the presence of a parallel δ-doped channel explains the significant difference between the experimental current–voltage characteristics from sample to sample by the difference in the conditions of formation of the potential difference U_{12} between the parallel channels [3M].

We assume the voltage $U_{12}(x) = \varphi_2(x) - \varphi_1(x)$ to be formed in our samples due to the perturbation of the potential φ1(x) in the near contact regions of the drain, $\varphi_D(d)$, and source, $\varphi_S(0)$. The potential in the source and drain regions determines, respectively, the channel depletion ($\varphi_2(0) - \varphi_S(0) = U_{12} < 0$) and enrichment ($\varphi_2(d) - \varphi_D(d) = U_{12} > 0$). At $\varphi_D(d) > \varphi_S(0)$, the concentration of the induced electrons in the QW channel increases, whereas at $\varphi_D(d) < \varphi_S(0)$ the channel becomes depleted. Assuming for definiteness that $U_{12}(x) = -\gamma\varphi_1(x)$ in the case of channel depletion, we find, according to (5), that

$$I_D = \frac{w\sigma_0}{d}\left(U_{SD} - \frac{\gamma}{U_T} \cdot \frac{U_{SD}^2}{2}\right). \qquad (6)$$

Expression (6) describes the sublinear I_D–U_{SD} characteristic on the assumption that the electron mobility μ_0 is field independent. We relate the maximum current value $I_{D\max}$ to the current saturation, which is clearly observed in the experiment and is caused by the change in the electron concentration in the channel: $I_{\text{sat}} = I_{D\max}$.

According to (6), the change in the electron concentration in the channel becomes as large as $\Delta N/N = 0.5$ at $I_{D\max}$. Accordingly, the electron drift velocity at $I_{D\max}$ reaches the values $v_{\max} = I_{D\max}/(0.5wN_{s0})$. The drift velocities $v_{\max}$, calculated using the experimental values of the saturation current I_{sat} for three pairs of samples. The estimated values of the electric field $E_C = v_{\max}/\mu_0$ corresponded to the current saturation. These rough estimates indicate a very large change in the electron concentration in the QW, which leads, despite the linear field dependence of the drift velocity, to the current saturation in the conduction channel of the $In_{0.53}Ga_{0.47}As/In_{0.52}Al_{0.48}As$ heterostructure [3M].

Sample 805 takes a particular place in these estimations. It has the following specific features: the structure with two InAs spacers and GaAs barriers was formed in such a menner as to implement the condition $\varphi_D(d) > \varphi_S(0)$; in addition, this sample exhibited an increase in the concentration, ΔN, with an increase in U_{SD} and a high saturation current I_{sat}. Note that the saturation currents in samples 804 and 805, which have similar initial concentrations N_{s0} in the QW, differ by a factor of 3. We assume the current saturation in sample 805 to be determined by the saturation of the drift velocity at the level of $v_{\max} \approx 5.1 \times 10^7$cm/s in the fields exceeding 4 kV/cm. These values of the drift velocity and threshold field are listed in Table 4 as estimates. The field E_C corresponding to the saturation in sample 794 is close to the critical field (4 kV/cm), above which the differential drift velocity in InGaAs becomes negative. Therefore, the decrease in the electron concentration can be accompanied by a decrease in the drift velocity and lead to negative conductivity and current instability in the QW. The experimentally observed current suppression in the samples of the 794 type (Fig. 12) is indicative of such current instability. The nature of this suppression may be similar to that observed in nanometer-gate transistors [4, 5, 15].

Table 4. Low-field mobility μ_{eksp}, saturation current I_{sat}, saturation drift velocity v_{sat} and E_C, electric field of current saturation

$In_{0,52}Al_{0,48}As/In_{0,53}Ga_{0,47}As/In_{0,52}Al_{0,48}As$ sample No.	μ_{eksp}, 10^3cm^2/(V·s)	I_{sat}, mA	v_{sat}, 10^7cm/s	E_C, 10^3V/cm
794	6,6	69	2,5	3,8
796	9,4	69	3,4	3,6
802	10	28	2,7	2,7
803	10	30	2,9	2,9
804	13,4	31	4,0	3,0
805	12,8	89	5,1	4,0

Electrons drift velocity in the $Al_{0.3}Ga_{0.7}As/GaAs/Al_{0.3}Ga_{0.7}As$ QW at high electric fields

Fig. 17 and Fig. 18 show the field dependences of electron drift velocity in modulate-doped $Al_{0.3}Ga_{0.7}As/GaAs$ structures with different QW widths. One can see that the field dependence $v_{dr}(E)$ in the QW is sublinear and have no region with the negative slope where $\sigma_d < 0$. It is worth to note that the threshold field for velocity saturation decreases about 3 times with increasing the QW width in a range of 10–30 nm (Fig. 18). These drift velocity field dependences are obtained from the experimental current–voltage characteristics $I(U)$ using the measured low-field sheet electron concentration N_s. Fig. 17 demonstrates the $v_{dr}(E)$ in the QW of the single heterojunction T-type structures. One can see that, at $E = 10$ kV/cm, the electron drift velocity exceeds the maximum saturated drift velocity in bulk GaAs by a factor of 1.5. This is in agreement with the predicted increase of drift velocity in a triangular QW. The triangular QW approximation gives the calculated ratio of $W_{bulk}/W_{QW} = 1.8$ for $z_0 = 6$ nm at $N_s = 2.6 \cdot 10^{12} cm^{-2}$ [2M]. Fig. 18 shows field dependences of the electron drift velocity in the double barrier $Al_{0.3}Ga_{0.7}As/GaAs/Al_{0.3}Ga_{0.7}As$ structures (A-, B**-, and C-type

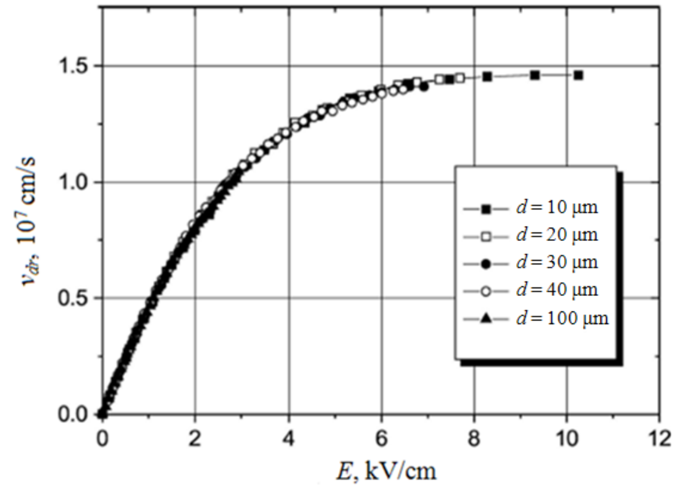

Fig. 17. Field dependences of the electron drift velocity vdr in the channel of modulation-doped single heterojunction $Al_{0.3}Ga_{0.7}As/GaAs$ structure (triangular QW, T***-type sample) with different spacing d between the contacts [2M].

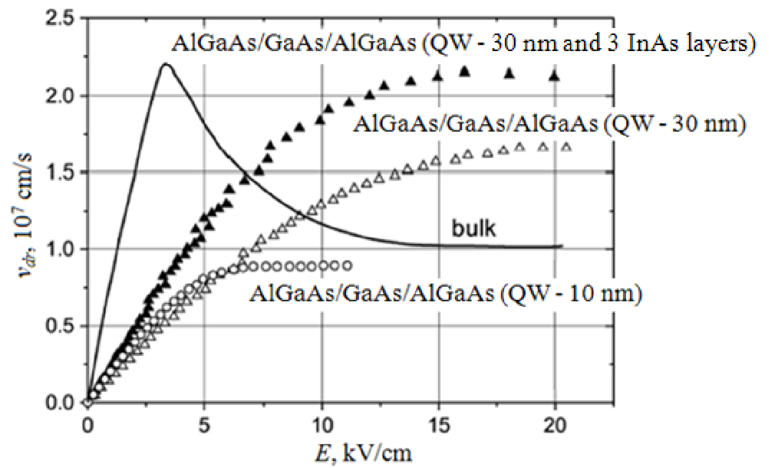

Fig. 18. Field dependences of the electron drift velocity v_{dr} in the double-barrier $Al_{0.3}Ga_{0.7}As/GaAs/Al_{0.3}Ga_{0.7}As$ structure with a different width of the GaAs QW: 30 nm in samples A and B** and 10 nm in sample C. The spacing between the contacts is d = 10 μm. Sample B** has three thin (1 ML InAs) phonon barriers inserted into the GaAs layer. The full curve represents the field dependence of the drift velocity in bulk GaAs [2M].

samples). In sample C with the narrow QW of width $L_z = 10$ nm, the drift velocity at electric fields of $E > 6$ kV/cm saturates and does not exceed the velocity in bulk GaAs. This is in agreement with the scattering rate estimation for a narrow QW. The velocity saturation takes place at $E \geq 5$ kV/cm. In samples A and B** with a wider QW ($L_z = 30$ nm), the predicted increase of the drift velocity over that in bulk material is observed. Velocity saturation takes place at $E > 12$ kV/cm. In sample A at $E = 15$ kV/cm, the drift velocity exceeds the saturated drift velocity in bulk by a factor of 1.6. The largest increase of the drift velocity is observed experimentally in sample B**. This structure contains three thin (1 monolayer of InAs) PO phonon barriers dividing the GaAs well into four narrow phonon wells. In papers [11, 19] it has been shown that the separation of the QW by thin InAs phonon walls and localization of the confined PO phonons in narrow phonon wells significantly decrease the electron–phonon scattering rate. At $E = 15$ kV/cm, the drift velocity in sample B** achieves 2.1×10^7 cm/s. Therefore, the experimental data confirm the predicted increase of the electron drift velocity in a moderately wide GaAs QW over the maximum saturated drift velocity in bulk GaAs. It is worth to note that similar experimental measurements of the drift velocity at high electric fields $E > 10$ kV/cm were performed in [4M]. These investigations have confirmed the increase of the drift velocity in the QW larger than 10 nm as compared to the saturated drift velocity in bulk GaAs [2M].

To summarize this section we can state that using of the strong direct current electrical pulses gave us the following results:

Experimentally it was found that the electron drift velocity dependence on the electric field strength of the AlGaAs/GaAs and AlGaAs/InGaAs/AlGaAs quantum wells is almost linear at low electric fields, and this dependence does not have any negative differential conductivity field. It has been demonstrated experimentally, that electron drift velocity in the quantum well of $Al_{0.3}Ga_{0.7}As/GaAs/Al_{0.3}Ga_{0.7}As$ heterostructure is 1.6×10^7 cm/s. Experiments had shown, that insertion of the InAs phonon barriers into the $Al_{0.3}Ga_{0.7}As/GaAs/Al_{0.3}Ga_{0.7}As$ heterostructures GaAs layer, can give a higher saturation of drift velocity value, which can reach the 2.1×10^7 cm/s. Also it was found that the insertion of the InAs phonon barriers into the $In_{0.52}Al_{0.48}As/In_{0.53}Ga_{0.48}As/In_{0.52}Al_{0.48}As$ heterostructure InGaAs layer (as well as at the two additional GaAs insertions into the InGaAs/InAlAs junction), saturated electron drift velocity increases to the 5×10^7 cm/s.

It has been demonstrated experimentally, that the optical polar phonon localisation in the phonon wells while inserting InAs barrier into the quantum well of the InAlAs/InGaAs/InAlAs heterostructure, can lead to the loss of the electron scattering while at the same time it will increase the electron mobility.

"General conclusions"

It was found experimentally that voltage–power sensitivity of asymmetrically shaped modulation–doped AlGaAs/GaAs microwave diodes increases up to 3 orders when the active area of the diode was gate–like metalized.

Voltage–power sensitivity of the microwave diodes made on the base of $Al_{0.28}Ga_{0.72}As/In_{0.15}Ga_{0.85}As/GaAs$ is twice as higher comparing to the $Al_{0.25}Ga_{0.75}As/GaAs$ diode.

It was also noticed that in AlGaAs/GaAs/AlGaAs heterojunction, drift velocity monotonically saturated at high (8–15 kV/cm) electric fields.

Experimentally it was found that saturated electron drift velocity in the AlGaAs/InGaAs/AlGaAs structures is 1.6×10^7 cm/s, and it is higher than that in the bulk GaAs (1×10^7 cm/s).

Experimental investigation has shown that insertion of the InAs phonon barriers into the quantum well nanostructures increases the saturation value of the electron drift velocity.

Also it is shown that electron drift velocity in the AlGaAs/GaAs/AlGaAs structures with InAs phonon barriers is higher (2.1×10^7 cm/s) compared to that of AlGaAs/GaAs/AlGaAs without InAs phonon barriers in the GaAs layer (1.6×10^7 cm/s).

Electron saturated drift velocity in $In_{0.52}Al_{0.48}As/In_{0.53}Ga_{0.48}As/In_{0.52}Al_{0.48}As$ heterojunction with InAs phonon barriers increases to the 5×10^7 cm/s, depending on the doping and insertions in the quantum well of the structure.

References

1. B. K. Ridley and N. A. Zakhleniuk, Hot electrons under quantization conditions: I. Kinematics // Journal of Physics: Condensed Matter. V. 8, No. 44, (1996), pp. 8525–8537
2. B. K. Ridley and N. A. Zakhleniuk, Hot electrons under quantization conditions: II. The Boltzman equation // Journal of Physics: Condensed Matter. V. 8, No. 44, (1996), pp. 8539–8552

3. B. K. Ridley and N. A. Zakhleniuk, Hot electrons under quantization conditions: III. Analytical results and new nonlinear regimes // Journal of Physics: Condensed Matter. V. 8, No. 44, (1996), pp. 8553–8581
4. W. J. Stillman, M. S. Shur, Closing the Gap: Plasma Wave Electronic Terahertz Detectors // Journal of Nanoelectronics and Optoelectronics, V. 2, (2007), p. 209
5. N. Dyakonova, A. Fatimy, J. Lusakowski, W. Knap, Room-temperature terahertz emission from nanometer field-effect transistors // Applied Physics Letters, V. 88, (2006), p. 141906
6. A. Juozapavičius, A. Ardaravičius, A. Sužiedėlis, A. Kozič, J. Gradauskas, J. Kundrotas, D. Seliuta, E. Širmulis, A. Ašmontas, G. Valušis, H.G. Roskos, K. Kohler, Microwave sensor based on modulation-doped GaAs/AlGaAs structure // Semiconductor Science and Technology, V. 19, No. 4, (2004), pp. S436–S439
7. S. Asmontas and A. Suziedelis, Microwave detector // International Journal Infrared and Millimeter Waves, V. 15, No. 3, (1994), pp. 525-538
8. V. Petkun, V. Kazlauskaitė, A. Sužiedėlis, Automatizuota bandinių voltamperinių charakteristikų matavimo sistema, naudojanti prietaisus, neturinčius universaliosios sąsajos // PFI 2006 metų mokslinės konferencijos darbai, (2006)
9. J. Pozela and A. Reklaitis, Solid-State Electronics V. 23, No. 9, (1980), pp. 927–933
10. J. Požela, K. Požela, V. Jucienė, Electrons scattering by interface polar optical phonons in double barrier heterostructures // Lithuanian Journal of Physics, V. 47, No. 1 (2007), p. 41–49
11. Ю. Пожела, К. Пожела, В. Юцене, Рассеяние электронов на захваченных поверхностных полярных оптических фононах в двухбарьерной гетероструктуре // Физика и Техника Полупроводников, том 41, вып. 9, (2007), сс. 1093-1098
12. L. Reggiani, Hot-Electron Transport in Semiconductors, Modena, (1994), p. 276
13. М. Шур, Современные приборы на основе арсенида галлия, Москва, (1991), с. 632
14. M. Tomizawa, K. Yokoyama, A. Yoshii, Hot-Electron Velocity Characteristics at AlGaAs/GaAs Heterostructures // IEEE Electron Device Letters, V. EDL-5, No. 11, (1984), pp. 464–465
15. Ю. Пожела, К. Пожела, В. Юцене, А. Сужеделис, А.С. Школьник, С.С. Михрин, В.С. Михрин, Взаимодействие электронов с локализованными в квантовой яме оптическими фононами // Физика и Техника Полупроводников, том 43, вып. 12, (2009), сс. 1634–1640
16. J. Požela, K. Požela, A. Shkolnik, A. Sužiedėlis, V. Jucienė, S. Mikhrin, V. Mikhrin, Hight-field electron mobility in InGaAs quantum wells // Physica Status Solidi C, V. 6, No. 12, (2009), pp. 2713–2715
17. T. Akazaki, K. Arai, T. Enoki, Y. Ishii, Improved InAlAs/InGaAs HEMT Characteristics by Inserting an InAs layer into the InGaAs Channel // IEEE Electron Device Letters, V. 13, No. 6, (1992), p. 325–327
18. Г.Б. Галиев, И.С. Васильевский, Е.А. Климов, В.Г. Мокеров, А.А. Черечукин, Влияние температуры роста спейсерного слоя на подвижность двухмерного электронного газа в

PHEMT-структурах // Физика и Техника Полупроводников, том 40, вып. 12, (2006), сс. 1479–1483
19. Ю. Пожела, К. Пожела, В. Юцене, С. Балакаускас, В.П. Евтихиев, А.С. Школьник, Ю. Стораста, А. Мекис, Повышение подвижности электронов в двухбарьерной гетероструктуре AlGaAs/GaAs/AlGaAs при введении в квантовою яму GaAs тонких InAs-барьеров для полярных оптических фононов // Физика и Техника Полупроводников, том 41, вып. 12, (2007), сс. 1460–1465

Scientific publications of author on the topic of the dissertation

1M. K. Požela, J. Požela, V. Jucienė, I.S. Vasil'evskii, G.B. Galiev, E.A. Klimov, A. Sužiedėlis, N. Žurauskienė, V. Stankevič, S. Keršulis and Č. Paškevič, Electron Transport in Modulation-Doped InAlAs/InGaAs/InAlAs Heterostructures in High Electric Fields // Acta Physica Polonica A, V. 119, No. 2, (2011), pp. 170–172
2M. J. Požela, K. Požela, A. Sužiedėlis, V. Jucienė, and Č. Paškevič, Saturated Electron Drift Velocity at high Electric Fields in AlGaAs/GaAs/AlGaAs Heterostructures // Lithuanian Journal of Physics, V. 50, No. 4, (2010), pp. 397–402
3M. I. S. Vasil'evskii, G. B. Galiev, Yu. A. Matveev, E. A. Klimov, J. Požela, K. Požela, A. Sužiedėlis, Č. Paškevič, and V. Jucienė; Electron Transport in an $In_{0.52}Al_{0.48}As/In_{0.53}Ga_{0.47}As/In_{0.52}Al_{0.48}As$ Quantum Well with a δ-Si Doped Barrier in High Electric Fields // Semiconductors, V. 44, No. 7, (2010), pp. 898–903.
4M. V. G. Mokerov, I. S. Vasil'evskii, G. B. Galiev, J. Požela, K. Požela, A. Sužiedėlis, V. Jucienė, Č. Paškevič, Drift Velocity of Electrons in Quantum Wells in High Electric Fields // Semiconductors, 2009, V. 43, No. 4, pp. 458–462
5M. A. Kozič, Č. Paškevič, A. Sužiedėlis, J. Gradauskas, S. Ašmontas, A. Szerling, H. Wrzesinska. Asymmetrically shaped pseudomorphic moduliation doped structure for microwave detection // Acta Physics Polonica A, V. 110, No 6, (2006), pp. 845–849.

Scientific Conferences

6M. A. Sužiedėlis, A. Kozič, Č. Paškevič, V. Petkun, J. Gradauskas, J. Požela, S. Ašmontas, H. Shtrikmann, V. Kisseliov, T. Anbinderis. Gate-Influenced Increase of Voltage Sensitivity in Asymmetrically Shaped 2DEG Microwave Diodes // An International Joint Conference of 4th ESA Workshop on Millimetre Wave Technology and Applications, Finland, Espoo, February 15-17, (2006), pp. 239-244.
7M. A. Kozič, Č. Paškevič, A. Sužiedėlis, J. Gradauskas, S. Ašmontas, A. Szerling, H. Wrzesinska. Asymmetrically shaped pseudomorphic moduliation doped structure for microwave detection // XXXV International School on the Physics of Semiconducting Compounds, Poland, Jaszowiec, June 17-23, (2006), p. 99

8M. S. Asmontas, J. Gradauskas, A. Suziedelis, A. Kozic, C. Paskevic, V. Kazlauskaite, and E. Sirmulis. Microwave to Terahertz Radiation Detection by Semiconductor Nanostructures, Proc. Tenth Annual Directed Energy Symposium, 5 - 8 November 2007, Huntsville, Alabama, USA, CD-ROM, (2007), pp. 813-826

9M. S. Ašmontas, J. Gradauskas, V. Nargelienė, Č. Paškevič, A. Sužiedėlis and E. Širmulis, Semiconductor nanostructures for microwave and terahertz radiation detection // Seoul, Korea, July 25 – 30, (2010) – ICPS

10M. K. Požela, J. Požela, A. Sužiedėlis, V. Jucienė, N. Žurauskienė, S. Keršulis, V. Stankevič, and Č. Paškevič, Electron Transport in Modulation-Doped InAlAs/InGaAs/InAlAs Heterostructures at High Electric Fields // Semiconductor Physics Institute, Center for Physical Sciences and Technology, Goštauto 11, Vilnius, Lithuania; 22-25 August, (2010) – 14 UFPS

11M. K. Požela, J. Požela, R. Raguotis, V. Jucienė, A. Sužiedėlis, S. Balakauskas, Č. Paškevič, Elektronų pernaša GaAs ir InGaAs kvantinėse duobėse stipriuose elektriniuose laukuose // pranešimas 38 Lietuvos nacionalinėje fizikos konferencijoje, Vilnius, 2009 birželis, 8-10 d.

Not included in the disseration

1N. A. Sužiedėlis, S. Ašmontas, J. Požela, J. Gradauskas, V. Nargelienė, Č. Paškevič, V. Derkach, R. Golovashchenko, E. Goroshko, V. Korzh and T. Anbinderis, Influence of Magnetic Field on Detection Properties of Planar Microwave Diodes // Acta Physics Polonica A, V. 119, No. 2, (2011), pp. 218–221

2N. A. Sužiedėlis, S. Ašmontas, J. Požela, J. Gradauskas, V. Nargelienė, Č. Paškevič, Influence of Magnetic Field on Detection Properties of Planar Microwave Diodes // Semiconductor Physics Institute, Center for Physical Sciences and Technology, Goštauto 11, Lithuania, 22-25 August, (2010) – 14 UFPS;

3N. Сужеделис А., Ашмонтас С., Пожела Ю., Градаускас И., Наргелене В., Пашкевич Ч., Влияние магнитного поля на детекционные свойства планарных микроволновых диодов на основе полупроводниковых селективно легированных структур // 20-я Международная Крымская конференция СВЧ-техника и телекоммуникационные технологии, Материалы конференции 13–17 сентября 2010г. Севастополь, Крым, Украина (2010), сс. 1027–1028 – CriMiCo

4N. G. B. Galiev, I. S. Vasil'evskii, E. A. Klimov, D. S Ponomorev, J. Požela, K. Požela, A. Sužiedėlis, V. Jucienė, Č. Paškevič, S. Keršulis and V. Stankevič, Electron mobility and high-field drift velocity enhancement in an InAlAs/InGaAs/InAlAs quantum well heterostructures // Proceedings of 19-th International Symposium: „Nanostructures: Physics and technology“, Ekaterinburg, Russia, June 20–25, (2011), pp. 57-58;

Short information about the author

Česlav Paškevič was born in the year 1981 in Rukainiai village of Vilnius district. He leaved Rukainiai secondary-school in 1999. In the same year he entered the Physics and Technology faculty of Vilnius Pedagogical University. Here in the year 2004 graduated from the physics and computer technology speciality and took bachelor's degree in physics and was given the qualification of physics teacher. There also continued his education in postgraduate studies in physics and astrophysics (IT technology) speciality, which successfully completed in the year 2006. After the Master degree studies, he started PhD studies in Vilnius University and Institute of Semiconductor Physics, where he continued his studies until 2010. Now he is a junior researcher in Semiconductor structures laboratory of the Electronics department at the Semiconductor Physics Institute of Center for Physical Sciences and Technology.

Reziumė

Disertacinis darbas susideda iš įvado, literatūros apžvalgos, tyrimo metodikos, dviejų eksperimentinių rezultatų pristatymo skyrių, pagrindinių išvadų, publikacijų sąrašo bei literatūros šaltinių.

Įvade yra pristatomi darbo aktualumas, tyrimo objektas, darbo tikslas, pagrindiniai darbo uždaviniai, tyrimo metodai, mokslinis naujumas, praktinė mokslinio darbo vertė, ginamieji teiginiai, mokslinio darbo rezultatų aprobavimas bei disertacijos struktūra.

Literatūros apžvalgoje yra apžvelgtas karštųjų krūvininkų sąlygotos elektrovaros susidarymas bei jos matavimo būdai (kontaktinis ir nekontaktinis). Pateikiamos nesimetriškai susiaurintos formos mikrobangų dioduose vykstančių procesų teorinės lygtys. Trumpai yra pristatomi įvairiatarpiai puslaidininkiniai dariniai ir juose vykstantys reiškiniai bei jų taikymas puslaidinkiniuose prietaisuose.

Antrame disertacijos skyriuje yra pateikta tyrimų metodika, kuri buvo naudojama moksliniame darbe. Yra aprašyti krūvininkų kaitinimo elektriniu lauku metodai: nuolatinės įtampos impulsų bei stipraus mikrobangų elektrinio lauko metodai. Yra pateikta įvairiatarpių darinių parametrų stipriuose elektriniuose laukuose matavimo schema. Taipogi yra aprašytas voltamperinių charakteristikų matavimas, kuris buvo naudojamas krūvininkų slinkio greičiui nustatyti rankiniu ir automatizuotu būdu.

Pateikiama automatizuoto voltamperinės charakteristikos matavimo sistemos struktūrinė schema. Yra trumpai aprašoma darbe naudojamų darinių gamyba nuo puslaidininkinio kristalo užauginimo iki kontaktų padarymo.

Trečiame darbo skyriuje buvo tirtos kelių puslaidininkinių darinių pagrindu pagamintų mikrobangų diodų be užtūros ir mikrobangų diodų su užtūra įtampos jautrio savybės. Buvo pastebėta, kad įvairių mikrobangų diodų detektavimo charakteristikos, stebimos mikrobangų elektriniame lauke, buvo kiekybiškai skirtingos. Įtampos jautrio esminis skirtumas buvo stebimas tiriant skirtingų struktūrų mikrobangų diodus, esant kambario temperatūrai bei esant skystojo azoto temperatūrai. Pastebėta, kad esant kambario temperatūrai, mikrobangų diodo be užtūros voltvatinis jautris tiesiškai priklauso nuo mikrobangų elektrinio lauko galios 2 mW – 150 mW ruože. Mikrobangų diodo su užtūra voltvatinio jautrio charakteristikų dinaminis diapazonas yra ribojamas mažesnės mikrobangų spinduliavimo galios, t.y., voltvatinis jautris tiesiškai priklauso nuo mikrobangų elektrinio lauko galios 1 μW – 0,2 mW ruože. Esant skystojo azoto temperatūrai, mikrobangų diodo be užtūros voltvatinė priklausomybė yra beveik tiesinė nuo 0,02 mW iki 40 mW mikrobangų elektrinio laukos galios ruože. Mikrobangų diodo su užtūra voltvatinė priklausomybė yra beveik tiesinė nuo 20 nW iki 1 μW mikrobangų elektrinio laukos galios ruože.

Ketvirtame darbo skyriuje yra pateikiami elektronų pernašos eksperimentiniai rezultatai. Trumpai aprašyti tirti bandiniai. Pateikti krūvininkų soties slinkio greičio tyrimo rezultatai elektriniuose laukuose. Pateikta eksperimento rezultatų priklausomybė nuo bandinių sudėties, ir parodyta, kad įterpiant plonus InAs sluoksnius į tirtą InAlAs/InGaAs/InAlAs darinį, eksperimento rezultatai gerėja. Buvo parodyta, kad įterpimas kvantinėje duobėje fononų sienelių žymiai mažina elektronų sklaidos spartą ir didina elektronų judrį kvantinėje duobėje. Tiriant krūvininkų slinkio greitį buvo pastebėta, kad InAlAs/InGaAs/InAlAs darinyje krūvininkų soties slinkio greitis gali gali padidėti iki 5 kartų lyginant su maksimaliu soties slinkio greičiu tūriniame GaAs, priklausomai nuo intarpų išsidėstymo tirtame darinyje. O AlGaAs/GaAs/AlGaAs darinio bandinio su įterptais InAs monosluoksniais elektronų soties slinkio greitis pasiekdavo $2,1\cdot10^7$ cm/s vertę.

Darbo pabaigoje yra apibendrinamas tiriamasis darbas ir pateikiami tokie rezultatai:

1) Eksperimentiškai buvo nustatyta, kad esant aktyviosios srities metalizuotai užtūrai, nesimetriškai susiaurintos formos selektyviai legiruotų AlGaAs/GaAs mikrobangų diodų jautris padidėja trimis eilėmis.
2) Mikrobangų diodų, pagamintų iš $Al_{0,28}Ga_{0,72}As/In_{0,15}Ga_{0,85}As/GaAs$ voltvatinis jautris yra dvigubai didesnis negu $Al_{0,25}Ga_{0,75}As/GaAs$ diodų.
3) Buvo stebėta, kad $Al_{0,3}Ga_{0,7}As/GaAs/Al_{0,3}Ga_{0,7}As$ dariniuose didinant elektrinį lauką, slinkio greitis monotoniškai įsisotina prie stiprių (8–15 kV/cm) laukų.
4) Eksperimentiškai gauta, kad $Al_{0,3}Ga_{0,7}As/GaAs/Al_{0,3}Ga_{0,7}As$ darinio elektronų soties slinkio greitis yra $1,6\cdot10^7$ cm/s, t. y. yra didesnis negu tūrinio GaAs elektronų soties slinkio greitis ($1\cdot10^7$ cm/s).
5) Eksperimentiškai parodyta, kad InAs fononų barjerų įterpimas į tirtų nanodarinių kvantines duobes, didina elektronų soties slinkio greičio reikšmę.
6) Eksperimentiškai nustatyta, kad $Al_{0,3}Ga_{0,7}As/GaAs/Al_{0,3}Ga_{0,7}As$ darinio su InAs fononų barjerais elektronų slinkio greitis ($2,1 \cdot 10^7$ cm/s) yra didesnis negu $Al_{0,3}Ga_{0,7}As/GaAs/Al_{0,3}Ga_{0,7}As$ darinio be InAs fononų barjerų GaAs sluoksnyje ($1,6 \cdot 10^7$ cm/s).
7) $In_{0,52}Al_{0,48}As/In_{0,53}Ga_{0,48}As/In_{0,52}Al_{0,48}As$ darinio su InAs fononų barjerais elektronų soties slinkio greitis padidėja iki $5\cdot10^7$ cm/s, priklausomai nuo legiravimo bei intarpų išsidėstymo darinio kvantinėje duobėje.

Literatūros sąraše yra pateikiami darbai, kurie buvo apžvelgti bei cituojami darbe.

Trumpos žinios apie autorių

Česlav Paškevič gimė 1981 m. Vilniaus rajone. 1999 m. baigė Rukainių vidurinę mokyklą. Tais pačiais metais įstojo į Vilniaus pedagoginio universiteto Fizikos ir technologijos fakultetą. Čia 2004 m. baigė Fizikos ir kompiuterinių technologijų specialybę ir įgijo fizikos bakalauro laipsnį bei buvo suteikta fizikos mokytojo kvalifikacija. Ten pat tęsė mokslus magistrantūros studijose studijuojant Fizikos ir astrofizikos (informacinių technologijų šakos) specialybėje, kurią sėkmingai baigė 2006 m. Iš karto po magistrantūros studijų įstojo į Vilniaus universiteto ir Puslaidininkių fizikos instituto doktorantūrą, kur tęsė mokslus iki 2010 m. Dabar dirba jaunesniuoju mokslo darbuotoju Fizinių ir technologijos mokslų centro Puslaidininkių fizikos instituto Elektronikos skyriaus Puslaidininkinių darinių laboratorijoje.